Spectral Vanishing Viscosity Method for Large-Eddy Simulation of Turbulent Flows

Richard Pasquetti[1]

An efficient spectral vanishing viscosity method for the large-eddy simulation of incompressible flows is proposed, both for standard spectral and spectral element approximations. The approach is integrated in a collocation spectral Chebyshev-Fourier solver and then used to compute the turbulent wake of a cylinder in a crossflow confined geometry (Reynolds number $Re = 3900$).

KEY WORDS: Large-eddy simulation; Spectral methods; Spectral vanishing viscosity; Wake flows; Turbulence.

1. INTRODUCTION

The spectral vanishing viscosity (SVV) method was introduced in the late 80's [24] in order to solve, with the spectral Fourier method, 1D non-linear conservations laws (typically, the inviscid Burgers equation). The non-periodic case was investigated later [16], using a Legendre polynomial approximation. In both cases the basic idea is to introduce a SVV term V_N, only active in the high frequency range, in order to stabilize the calculations while preserving the exponential rate of convergence of the discrete solution towards the fully converged spectral approximation of the exact one. Let us follow [16] and denote $\Lambda = (-1, 1)$, $P_N(\Lambda)$ the space of polynomials of maximum degree N defined on Λ, $u_N(x) \in P_N(\Lambda)$ the polynomial approximation of the exact solution $u(x)$ and $\{L_k\}_{k \geqslant 0}$ the set of Legendre polynomials. Then the SVV term is written as: $V_N = \epsilon_N \partial_x(Q_N(\partial_x u_N))$, where ϵ_N is a $O(N^{-1})$ coefficient and where Q_N is a "spectral viscosity operator" such that: $\forall \phi, \quad \phi = \sum_{k=0}^{\infty} \hat{\phi}_k L_k, \quad Q_N \phi \equiv \sum_{k=0}^{N} \hat{Q}_k \hat{\phi}_k L_k$, where

[1]Lab. J.-A. Dieudonné, UMR CNRS 6621, Université de Nice-Sophia Antipolis, Parc Valrose, 06108 Nice Cedex 02, FR. E-mail: richardpasquetti@unice.fr

$\hat{Q}_k = 0$ if $k \leqslant m_N$ and $0 < \hat{Q}_k \leqslant 1$ if $k > m_N$, with e.g. $m_N = \sqrt{N}$ and $\hat{Q}_k = \exp(-(k-N)^2/(k-m_N)^2)$. For non-linear scalar 1D conservation laws theoretical studies state that $m_N \sim N^{q/4}$, with $q < 1$, $\epsilon_N \sim N^{-1}$ and that $1 - (m_N/k)^4 \leqslant \hat{Q}_k \leqslant 1$ [16], but up to our knowledge such results are not yet available for the Navier-Stokes (NS) equations. Refinements of the SVV method have later on been suggested and spectrally vanishing super/hyperviscosity methods have also been proposed (see [9, 14] and related works).

The idea of using the SVV method for the large eddy simulation (LES) of turbulent flows was introduced in [11]. In our case we used the SVV method to stabilize a Defiltering-Transport-Filtering algorithm [18], i.e., an Approximate Deconvolution Method (see e.g., [1, 23]) in a semi-Lagrangian framework, and also observed that using the SVV method alone could yield satisfactory results [20]. Just like scale similarity models [6], approximate deconvolution methods are indeed source of numerical instabilities and so require complementary terms for stabilization. Thus, the scale similarity model is usually completed with an eddy viscosity term [6] and in [1] the evolution equations are supplemented by a relaxation regularization based on a secondary filter. Nevertheless, when spectral methods are concerned it is first of all required to preserve the exponential rate of convergence of the numerical approximation and, precisely, the SVV method shows this nice property.

Some differences can be observed in the implementation of the SVV method when the computational domain is no-longer 1D or when coordinate transforms are involved. Extensions of the pioneering works [24, 16] may be found in [8] and [10]. In [8], where again the periodic case is investigated, the SVV term is written: $V_N = \epsilon_N \sum_{i,j=1}^{d} \partial_{ij}^2 Q_N^{i,j} * u_N$ (see Eq. 1.2a), where d is the space dimension and the $Q_N^{i,j}$ a family of spherically symmetric viscosity kernels with monotonically increasing Fourier coefficients. In [10], the additional viscous term is for a 2D problem written, with slightly different notations: $V_N = \sum_{i,j=1}^{2} \epsilon_N^{ij} \partial_j (Q_N^{ij} (\partial_i u_N))$ (see Eq. 3.8), but in practice (see Sec. 4), $\epsilon_N^{ij} = \delta_{ij} \epsilon_N$ and $Q_N^{ij} = \delta_{ij} Q_N$ (δ_{ij}, Kronecker symbol). In [11] a 2D kernel Q_N is defined as the tensorial product of 1D kernels: $Q_N = \prod_{i=1}^{2} Q_{N_i}^i$ (see Eq. 11). For us we have also investigated this problem and used in the simplest case of a d-dimensional scalar equation $V_N = \sum_{i=1}^{d} \epsilon_{N_i} \partial_i (Q_{N_i}^i (\partial_i u_N))$ (see Sec. 2 for notations) and for a spectral element approximation we have recently proposed an efficient implementation of the SVV method [26].

In Sec. 2 we explain how to implement the SVV method in spectral NS solvers, considering first the standard collocation method and then the spectral element approximation. The SVV formulation proposed in [26] appears then quite natural. In Sec. 3 we focus on the computation of

turbulent wakes. First we describe our SVV stabilized NS solver before showing some quantitative results for the turbulent wake of a cylinder in a crossflow confined geometry (Reynolds number $Re = 3900$).

2. EFFICIENT SVV METHOD FOR NS SOLVERS

In dimensionless form the unsteady incompressible NS equations read:

$$D_t\boldsymbol{u} = -\nabla p + \nu\Delta\boldsymbol{u} \tag{1}$$
$$\nabla.\boldsymbol{u} = 0$$

where $\boldsymbol{u}$ is the velocity, p a pressure term, $\nu > 0$ the dimensionless viscosity (inverse of the Reynolds number), t the time variable and $D_t = \partial_t + \boldsymbol{u}.\nabla$ the material derivative. Such PDEs should be associated to suitable initial and boundary conditions to yield a well-posed NS problem. Hereafter, for the sake of simplicity we consider Dirichlet conditions. To solve the NS system different ways are possible (see, e.g., [5, 22]): Fractional step methods are among the favorite ones, but it is also classical, after the time discretization, to set up a Poisson equation for the pressure or to directly address the so-called generalized Stokes problem, that one can iteratively solve, at each time-cycle, by using an Uzawa algorithm. In any cases, efficient NS solvers make use of efficient elliptic solvers to compute, at a given time or at a given step of an iterative process, the pressure or one of the components of the velocity.

Thus, assume that the time derivative is discretized by using a Backward Euler of order Q (BEQ) scheme, that the non-linear convective term is treated explicitly and that the linear viscous term is treated implicitly. Then a fractional step method leads to compute, at each time cycle, a provisional velocity $\boldsymbol{u}^*$ such that each of its components, say u^*, solves the scalar semi-discrete problem:

$$(\nu\Delta - \alpha_0\delta t^{-1})\,u^* = f^{n+1} \qquad \text{in } \Omega$$
$$u^* = u_\Gamma(t_{n+1}) \quad \text{on } \Gamma \tag{2}$$

where Ω is the computational domain, Γ its boundary, n the time index, δt the time-step, α_0 a coefficient associated to the finite difference approximation of $\partial_t u^*$ and f^{n+1} a source term at time t_{n+1}.

At this point our goal is to propose an efficient implementation of the SVV method, i.e., that preserves the spectral accuracy, provides stability and minimizes the additional computational cost. This can be achieved by combining the viscous term of the NS equations with the SVV term, i.e., the diffusion term of Eq. (2) and the SVV term V_N, that we have first

to define precisely. Hereafter we discern our implementation of the SVV method for standard spectral methods and for a spectral element approximation, in an effort in the latter case to introduce a symmetric bilinear form even when arbitrary mappings are involved.

Standard spectral collocation method: We assume that the computational domain $\Omega = \Lambda^d$ (d: space dimension) and denote by: (i) $P_N(\Omega)$, the space of the polynomials of maximum degree N_i in x_i direction, with $N = (N_1, \ldots, N_d)$, (ii) Ω_N (Γ_N), the inner (boundary) Legendre or Chebyshev Gauss-Lobatto collocation points, (iii) $u_N \in P_N(\Omega)$ the polynomial approximation we are looking for (we omit the superscript $*$ for the sake of simplicity in the notations). As discussed in [26], in order to provide additional viscous fluxes when and only when it is required we define V_N as follows:

$$V_N \equiv \nabla \cdot \epsilon_N Q_N(\nabla u_N), \quad \epsilon_N Q_N \equiv diag\{\epsilon_{N_i} Q_{N_i}^i\}_{i=1}^d, \tag{3}$$

so that: $V_N = \sum_{i=1}^d \epsilon_{N_i} \partial_i(Q_{N_i}^i(\partial_i u_N))$, where $Q_{N_i}^i$ is the 1D spectral viscosity operator such that the $\hat{Q}_k^i$ act on the spectrum of the Legendre or Chebyshev expansion with respect to x_i.

Combining the viscous and SVV terms one can express the following SVV modified elliptic problem: Find $u_N \in P_N(\Omega)$ such that:

$$\begin{aligned} (\nu \Delta_{SVV} - \alpha_0 \delta t^{-1}) u_N &= f_N^{n+1} &\quad \text{in } \Omega_N \\ u_N &= u_\Gamma &\quad \text{on } \Gamma_N \end{aligned} \tag{4}$$

with: $\Delta_{SVV} \equiv \nabla \cdot S_N \nabla$, $\quad S_N \equiv \mathcal{I} + \nu^{-1} \epsilon_N Q_N$,
where $\mathcal{I}$ is the identity operator.

Problem (4) can be handled as a standard elliptic problem. Moreover, setting up the operator S_N is easy, because applying $S_{N_i}^i \partial_i$, where $S_{N_i}^i = 1 + \nu^{-1} \epsilon_{N_i} Q_{N_i}^i$, corresponds to a multiplication by a SVV modified differentiation matrix.

Spectral element approximation: Starting from the result obtained for the standard spectral method we are led to introduce a SVV modified viscous term:

$$(\Delta_{SVV} u_N, v_N) = (S_N(\nabla u_N), \nabla v_N) + B.T. \tag{5}$$

with $(.,.)$ denoting the $L^2(\Omega)$ inner product, $B.T.$ for Boundary Term and where $v_N \in P_N(\Omega)$ denotes some test function. For Dirichlet boundary conditions no difficulty arises with the boundary term. For Neumann or Robin conditions we in fact use the boundary term obtained for $S_N = \mathcal{I}$ (i.e., the usual boundary term), the resulting approximation being also

spectrally vanishing. If no mapping is involved, thanks to the L^2-orthogonality of the Legendre polynomials in Λ^d such a viscous term can be made symmetric:

$$(S_N(\nabla u_N), \nabla v_N) = (S_N^{1/2}(\nabla u_N), S_N^{1/2}(\nabla v_N)), \tag{6}$$

with $S_N^{1/2}$, in 1D, such that for $\phi = \sum_{k=0}^{\infty} \hat{\phi}_k L_k$ we have $S_N^{1/2}\phi = \sum_{k=0}^{N} \sqrt{\hat{S}_k} \hat{\phi}_k L_k$ where $\hat{S}_k = 1 + \nu^{-1}\epsilon_N \hat{Q}_k$.

In the framework of a spectral element approximation each spectral element, say ω, is however the image by a mapping, say f, of the reference domain $\Omega = \Lambda^d$. We are then led to introduce the following SVV modified viscous term:

$$(S_N(\nabla u_N), \nabla v_N)_{L^2(\omega)} \equiv (J\tilde{G}^T S_N(\tilde{\nabla}\tilde{u}_N), \tilde{G}^T \tilde{\nabla}\tilde{v}_N)_{L^2(\Omega)} \tag{7}$$

where the superscript $\tilde{\ }$ means "with respect to the variables of the reference domain", with the superscript T for "transposition", G for the Jacobian matrix of f^{-1} and $J > 0$ for the Jacobian of f. Such a viscous term can no-longer be made symmetric, except if the spectral element is only stretched in each spatial direction. In order to use efficient solvers for the final algebraic system it is however of interest to handle a symmetric bilinear form. This is why we suggest to use the SVV modified viscous term:

$$(S_N^{1/2}(\nabla u_N), S_N^{1/2}(\nabla v_N))_{L^2(\omega)} \equiv (J\tilde{G}^T S_N^{1/2}(\tilde{\nabla}\tilde{u}_N), \tilde{G}^T S_N^{1/2}(\tilde{\nabla}\tilde{v}_N))_{L^2(\Omega)}. \tag{8}$$

Such a term is clearly dissipative since:

$$J\tilde{G}^T S_N^{1/2}(\tilde{\nabla}\tilde{u}_N) \cdot \tilde{G}^T S_N^{1/2}(\tilde{\nabla}\tilde{v}_N) = [S_N^{1/2}(\tilde{\nabla}\tilde{u}_N)]^T \tilde{G} J\tilde{G}^T S_N^{1/2}(\tilde{\nabla}\tilde{v}_N)$$

where the matrix $\tilde{G}J\tilde{G}^T$ is positive definite.

If no SVV term is added then $S_N = \mathcal{I}$ and one recovers the usual viscous term. If the mapping resumes to stretching then the symmetric and non-symmetric bilinear forms are identical. The efficiency of this SVV spectral element formulation has not yet been carefully verified for LES, but in [26] we have numerically checked that the rate of convergence was exponential and that the stabilization effect was effective for the 2D wake of a cylinder at a Reynolds number $Re = 1000$.

Remark: In the frame of collocation methods, if the computational domain is the image by a mapping f of the reference domain, then, as in Eq. (7), it is relevant to use $S_N(\nabla u_N) \equiv \tilde{G}^T S_N(\tilde{\nabla}\tilde{u}_N)$.

3. SVV BASED LES OF TURBULENT WAKES

Firstly, we briefly describe the numerical method that we have developed for the computation of wakes in a channel like domain and the SVV implementation. Then, we give some quantitative results for the wake of a cylinder embedded in such a channel. Comparisons are provided with results obtained for a classical benchmark (see e.g. [12, 13]): the wake of a cylinder at Reynolds number $Re = 3900$ in an open domain.

Numerical method: Along the streamwise direction we use a domain decomposition technique to efficiently handle the elongated geometries typically encountered when studying wake type flows. In each subdomain we use Chebyshev polynomials in the x-streamwise and y-cross-flow directions and Fourier expansions in the z-spanwise homogeneous direction. Thanks to the decoupling of the Fourier modes, we thus essentially solve 2D problems with a Chebyshev collocation method.

The time-scheme is second order accurate and makes use of 3 steps: a transport step, to handle the convective term, a diffusion step, to handle the SVV modified viscous term and a projection step, to finally obtain a divergence-free velocity field. As explained in previous Section, the SVV stabilization technique is implemented in the diffusion step.

Transport step: A BE2 approximation ($\alpha_0 = 3/2, \alpha_1 = -2, \alpha_2 = 1/2$) of the material derivative yields:

$$D_t \boldsymbol{u}(t_{n+1}) = \frac{1}{\delta t}\left(\alpha_0 \boldsymbol{u}^{n+1} + \sum_{q=1}^{q=2}\alpha_q \tilde{\boldsymbol{u}}^{n+1-q}\right) + O\left(\delta t^2\right) \qquad (9)$$

with $\boldsymbol{u}^{n+1} \approx \boldsymbol{u}(\boldsymbol{x}, t_{n+1})$ and $\tilde{\boldsymbol{u}}^{n+1-q} \approx \boldsymbol{u}(\boldsymbol{\chi}(\boldsymbol{x}, t_{n+1}; t_{n+1-q}), t_{n+1-q})$, where $\boldsymbol{\chi}(\boldsymbol{x}, t_{n+1}; t)$ solves the characteristics equation. In order to avoid high order interpolations in space we use an "Operator Integration Factor" (OIF) Semi-Lagrangian method [15, 5, 25]. The $\tilde{\boldsymbol{u}}^{n+1-q}$ are thus determined as the solutions of two auxiliary transport problems for which we use an explicit scheme with large absolute stability region (RK4 scheme) with, if necessary, sub-time cycling.

Diffusion step: At each time t_{n+1} one computes a provisional velocity which solves the following semi-discrete equation:

$$\left(\nu \Delta_{SVV} - \frac{\alpha_0}{\delta t}\right)\boldsymbol{u}^* = \boldsymbol{f}^{n+1} \quad \text{in } \Omega \qquad (10)$$

with appropriate boundary conditions, e.g., $\boldsymbol{u}^*|_\Gamma = \boldsymbol{u}^{n+1}|_\Gamma = \boldsymbol{u}_\Gamma$, and:

$$\boldsymbol{f}^{n+1} = \frac{1}{\delta t}\sum_{q=1}^{q=2}\alpha_q \tilde{\boldsymbol{u}}^{n+1-q} + \nabla p^n.$$

This problem is solved by using a direct method (the "diagonalization technique", see e.g., [22]), so that the SVV stabilization requires no additional computational effort per time-step.

To model the bluff body we use an original "pseudo-penalty technique". It consists in preserving only the pressure contribution to the source term of Eq. (10) inside the obstacle. This is formally equivalent to using a penalization technique with a $O(\delta t^{-1})$ penalization coefficient. Moreover, to take more precisely into account the position of the bluff body, we use a local averaging of the characteristic function, e.g., in the spirit of VOF (volume of fluid) methods in the context of free surface flows. Of course, spectral accuracy gets lost. Here we simply assume that the phenomenon remains local, but one may think that related approaches, as e.g. developed in [7], will allow to recover it (preliminary results in [19]).

Projection step: To compute a divergence-free velocity field we solve the Darcy problem:

$$\boldsymbol{u}^{n+1} + \nabla\varphi = \boldsymbol{u}^* \text{in } \Omega$$
$$\nabla \cdot \boldsymbol{u}^{n+1} = 0 \text{in} \Omega \qquad (11)$$
$$\boldsymbol{u}^{n+1} \cdot \boldsymbol{n} = \boldsymbol{u}_\Gamma \cdot \boldsymbol{n} \text{on } \Gamma$$

where $\boldsymbol{n}$ is the outwards unit vector orthogonal to Γ and then the pressure field is updated: $p^{n+1} = p^n + \alpha_0 \varphi / \delta t$.

To solve the Darcy problem we use a *unique grid* $P_N - P_{N-2}$ strategy [2, 3], but to enforce the natural C^1 continuity of the pressure at the subdomain-interfaces we use, in each subdomain Ω^s, $1 \leqslant s \leqslant S$, the pressure polynomial space $P_{N'}(\Omega^s)$ such that $N' = (N_1 - 1, N_2 - 2)$ if $s = 1$ or $s = S$ (first and last subdomains) and $N' = (N_1, N_2 - 2)$ for $1 < s < S$. This yields a well-posed problem (the pressure is however defined up to a constant) and allows the velocity and vorticity fields to be continuous at the subdomain interfaces. More details can be found in [4].

Cylinder wake ($Re = 3900$): The characteristic parameters of the computations are the following: Domain: $\Omega = (-6.5, 17.5) \times (-4, 4) \times (-2, 2)$, with a cylinder of unit diameter and centered at $x = y = 0$; Boundary conditions: free-slip conditions at $y = \pm 4$, constant velocity ($u_x = 1$) at $x = -6.5$ (inlet), "advection" at the mean flow velocity at $x = 17.5$ (outlet); Number of subdomains: $S = 5$, with interfaces located at $x = \{-0.5, 2.5, 6.5, 11.5\}$; Polynomial approximation degrees: $N_1 = 60$, $N_2 = 120$ in x and y directions, respectively; Number of Fourier grid points: $N_F = 60$; SVV parameters: $m_N = N/2$ and $\epsilon_N = 1/N$.

Qualitative results may be found in [4] and a sensitivity study with respect to the SVV parameters in [21]. Here we restrict ourselves to quantitative results and moreover give some comparisons with the experiments
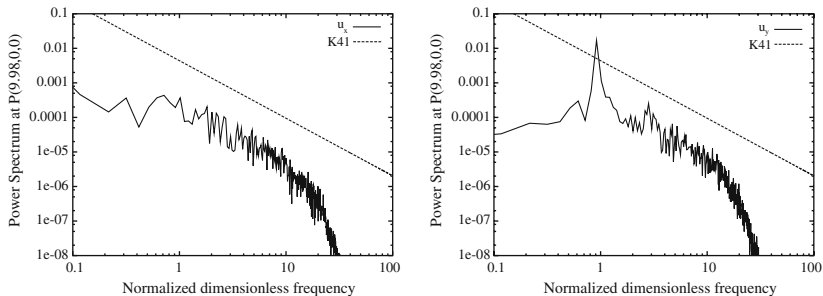
Fig. 1. Power spectra of u_x (left) and u_y (right) from history plots at $P(9.98, 0, 0)$. The dimensionless frequency is normalized with $St = 0.2$.

of Ong & Wallace [17], Lourenco & Shih (from [12]) and Williamson & Govardhan (from [13]). However, it must be kept in mind that although similar the physical problems are actually different due to the crossflow confinement of our flow.

One-dimensional energy spectra: Fig. 1 shows power spectra of the x and y components of the velocity, as computed from history plots at the point $P(9.98, 0, 0)$ in the time interval $(100, 250)$. Via the Taylor hypothesis, these power spectra should be in agreement with Kolmogorov theory ("K41 theory"), i.e., should show the characteristic $k^{-5/3}$ slope in the inertial range. As in [12] (see Fig. 10) or in [13] one observes an inertial range extending approximatively half a decade. The Strouhal number, characteristic of the vortex shedding phenomenon, is clearly pointed out by the cross-flow component: We find $St \approx 0.2$. The non-represented power spectrum of the z-component is also in good agreement with the K41 theory.

Mean flow: In Fig. 2 (left) we show profiles of the time averaged x-component of the velocity at different abcissa beyond the very near wake. The flow quantities were averaged in the time interval $(100, 250)$ but also in spanwise direction. Comparisons are done with the experimental measurements of Ong & Wallace [17]. Comparisons are also possible with the Fig. 15 of [12] or with the Fig. 12 of [13]. Especially, at the centerline the agreement with the DNS [13] is good. The disagreement for $|y| \gtrsim 1$ clearly results from the confinement of the flow. In Fig. 2 (right) we have plotted the variations of $\langle u_x \rangle$ in streamwise direction. Comparisons are here done with the experiments of Lourenco & Shih, Williamson & Govardhan and Ong & Wallace. The flow regimes obtained in the two first experiments are clearly different. The second compares better with what we have obtained, with a smooth variation of $\langle u_x \rangle$ behind the cylinder and a longer recirculation region. As a result it is not relevant to pro-
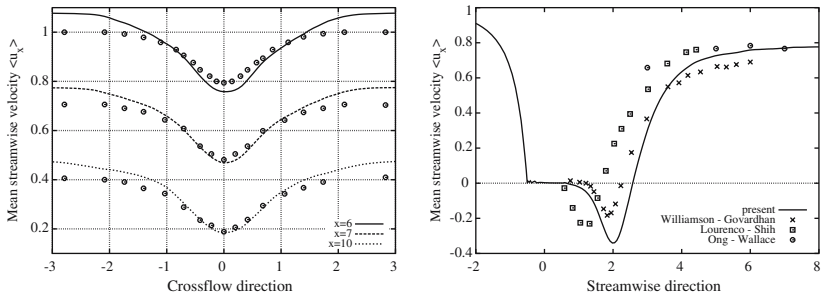
Fig. 2. Mean variations of u_x vs crossflow (left) and streamwise (right) directions. Experimental results from Lourenco & Shih (squares), Williamson & Govardhan (crosses) and Ong & Wallace (circles). For the computation the exact locations of the profiles are at the grid-point abcissa $x = 5.98$, $x = 6.96$ and $x = 9.98$.

vide as in [12, 13] comparisons with the experiments of Lourenco & Shih. One may suspect that the flow regime that we have obtained is induced by the crossflow confinement, but this point remains unclear. Concerning the SVV technique, we have checked that the recirculation length is slightly shortened when the SVV parameter m_N is increased or when ϵ_N is decreased, but the x-variation of $\langle u_x \rangle$ remains as in the experiment of Williamson & Govardhan.

Turbulence statistics: In Fig. 3 we present profiles of the Reynolds stresses $\langle u_x'^2 \rangle$ and $\langle u_x' u_y' \rangle$ (superscript ' for deviation) and compare them to the experimental results of Ong & Wallace. The computed stresses look similar to the experimental ones but are clearly greater. Comparisons are possible with the Fig. 16 and 17 of [12] or with the Fig. 13 of [13], which show better agreements with the experiment, although the DNS (case I) [13] overestimates $\langle u_x'^2 \rangle$ at $x = 4$. From the crossflow confinement increases
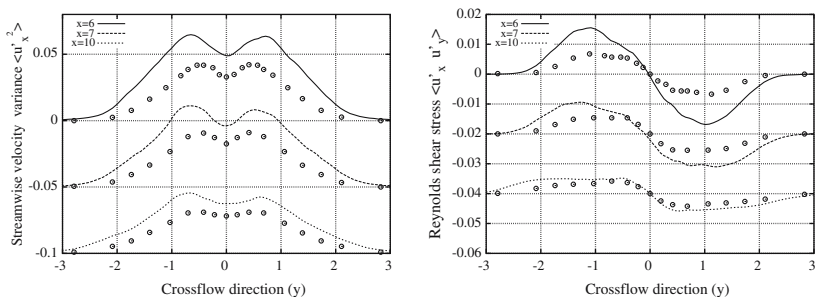
Fig. 3. Reynolds stresses $\langle u_x'^2 \rangle$ and $\langle u_x' u_y' \rangle$ vs crossflow direction. Comparisons with the experiments of Ong & Wallace.

of the Reynolds stresses were expected, but new investigations (numerical or experimental) would be needed to validate their amplitudes. Moreover, a streamwise shift induced by different very near wake flows should be suspected.

ACKNOWLEDGMENTS

REFERENCES

1. Adams, N. A., and Stolz, S. (2002). A subgrid-scale deconvolution approach for shock capturing, *J. Comput. Phys.* **178**, 391–426.
2. Azaiez, M., Fikri, A., and Labrosse, G. (1994). A unique grid spectral solver of the nD Cartesian unsteady Stokes system. Illustrative numerical results, *Finite Elem. Anal. Des.* **16**(3–4), 247–260.
3. Botella, O. (1997). On the solution of the Navier-Stokes equations using Chebyshev projection schemas with third order accuracy in time. *Comput. Fluids* **26**(2), 107–116.
4. Cousin, L., and Pasquetti, R. (2004). High-order methods for the simulation of transitional to turbulent wakes, In Lu, Y., Sun, W., and Tang, T. (eds.), *Advances in Scientific Computing and applications*, Science Press Beijing/New York.
5. Deville, M. O., Fischer, P. F., and Mund, E. H. (2002). High-order methods for incompressible flows, Cambridge University Press.
6. Gatsky, T. B., Hussaini, M. Y., and Lumley, J. L. (1996). Large Eddy Simulation, In Ferziger, J. H. (ed.), *in* Simulation and modeling of turbulent flows, *ICASE/LaRC Series in Computational Science and Engineering*, Oxford University Press, pp. 109–154.
7. Gottlieb, D., and Shu, C. W. (1997). On the Gibbs phenomenon and its resolution, *SIAM Rev.* **39**(4), 644–668.
8. Chen, G. Q., Du, Q., and Tadmor, E. (1993). Spectral viscosity approximations to multidimensional scalar conservations laws, *Math. of Comput.* **204**, 629–643.
9. Guo, B., Ma, H., and Tadmor, E. (2001). Spectral vanishing viscosity method for nonlinear conservation laws, SIAM J. Numer. Anal. **39**(4), 1254–1268.
10. Kaber, O. S. M. (1995). A Legendre pseudo-spectral viscosity method, *J. Comput. Phys.* **128**(1), 165–180.
11. Karamanos, G. S., and Karniadakis, G. E. (2000). A spectral vanishing viscosity method for large-eddy simulation, *J. Comput. Phys.* **163**, 22–50.
12. Kravchenko, A. G., and Moin, P. (2000). Numerical studies of flow over a circular cylinder at $Re = 3900$, *Phys. Fluids* **12**(2), 403–417.
13. Ma, X., Karamanos. G. S., and Karniadakis, G. E. (2000). Dynamic and low-dimensionality of a turbulent near wake, *J. Fluid Mech.* **410**, 29–65.
14. Ma, H. (1998). Chebyshev-Legendre superspectral viscosity method for non linear conservation laws, *SIAM J. Numer. Anal.* **35**(3), 893–908.
15. Maday, Y., Patera, A. T., and Ronquist, E. M. (1990). An operator-integration-factor splitting method for time-dependent problems: application to incompressible fluid flow, *J. of Sci. Comp.* **5**(4), 263–292.

Spectral Vanishing Viscosity Method

16. Maday, Y., Kaber, S. M. O., and Tadmor, E. (1993). Legendre pseudo-spectral viscosity method for nonlinear conservation laws, *SIAM J. Numer. Anal.* **30**(2), 321–342.

17. Ong, L., and Wallace, J. (1996). The velocity field of the turbulent very near wake of a circular cylinder, *Experiments in fluids* **20**, 441–453.

18. Pasquetti, R., and Xu, C. J. (2002). High-order algorithms for large eddy simulation of incompressible flows, *J. Sci. Comp.* **17**(1–4), 273–284.

19. Pasquetti, R. (2004). On inverse methods for the resolution of the Gibbs phenomenon, *J. of Comput. and Appl. Math.* **170**, 303–315.

20. Pasquetti, R. (2005). High-order LES modeling of turbulent incompressible flow, *C.R. Acad. Sci. (Mécanique)* **333**, 39–49.

21. Pasquetti, R. (in press). Spectral vanishing viscosity method for LES: sensitivity to the SVV control parameters, *J. of Turbulence*.

22. Peyret, R. (2001). *Spectral Methods for Incompressible Flow, Applied Mathematical Sciences* 148, Springer.

23. Stolz, S., and Adams, N. A. (1999). An approximate deconvolution procedure for large-eddy simulation, *Phys. Fluids* **11**(7), 1699–1701.

24. Tadmor, E. (1989). Convergence of spectral methods for nonlinear conservation laws, *SIAM J. Numer. Anal.* **26**(1), 30–44.

25. Xu, C. J., and Pasquetti, R. (2001). On the efficiency of semi-implicit and semi-Lagrangian spectral methods for the calculation of incompressible flows, *Inter. J. Numer. Meth. Fluids* **35**, 319–340.

26. Xu, C. J., and Pasquetti, R. (2004). Stabilized spectral element computations of high Reynolds number incompressible flows, *J. Comput. Phys.* **196**(2), 680–704.